

## Single mode interband cascade lasers based on lateral metal gratings

Robert Weih, Lars Nähle, Sven Höfling, Johannes Koeth, and Martin Kamp

Citation: [Applied Physics Letters](#) **105**, 071111 (2014); doi: 10.1063/1.4893788

View online: <http://dx.doi.org/10.1063/1.4893788>

View Table of Contents: <http://scitation.aip.org/content/aip/journal/apl/105/7?ver=pdfcov>

Published by the [AIP Publishing](#)

---

### Articles you may be interested in

[Corrugated-sidewall interband cascade lasers with single-mode midwave-infrared emission at room temperature](#)  
Appl. Phys. Lett. **95**, 231103 (2009); 10.1063/1.3272676

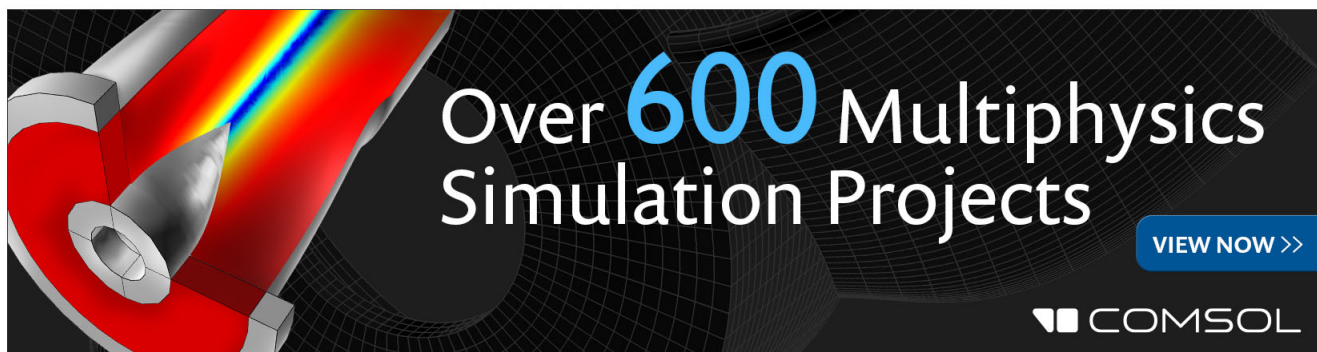
[Widely tunable distributed-feedback lasers with chirped gratings](#)  
Appl. Phys. Lett. **94**, 161102 (2009); 10.1063/1.3123813

[Single-mode distributed-feedback interband cascade laser for the midwave infrared](#)  
Appl. Phys. Lett. **88**, 191103 (2006); 10.1063/1.2202640

[High-performance operation of single-mode terahertz quantum cascade lasers with metallic gratings](#)  
Appl. Phys. Lett. **87**, 181101 (2005); 10.1063/1.2120901

[1.55  \$\mu\text{m}\$  single mode lasers with complex coupled distributed feedback gratings fabricated by focused ion beam implantation](#)  
Appl. Phys. Lett. **75**, 1491 (1999); 10.1063/1.124732

---

The advertisement features a 3D cutaway simulation of a laser component with a rainbow-colored light beam. The text 'Over 600 Multiphysics Simulation Projects' is prominently displayed in white and blue. A blue button with the text 'VIEW NOW >>' is located in the bottom right corner. The COMSOL logo is positioned at the bottom right of the image.

Over **600** Multiphysics  
Simulation Projects

[VIEW NOW >>](#)

COMSOL

## Single mode interband cascade lasers based on lateral metal gratings

Robert Weih,<sup>1</sup> Lars Nähle,<sup>2</sup> Sven Höfling,<sup>1,a)</sup> Johannes Koeth,<sup>2</sup> and Martin Kamp<sup>1</sup>

<sup>1</sup>*Technische Physik, Physikalisches Institut and Wilhelm Conrad Röntgen-Research Center for Complex Material Systems, Universität Würzburg, Am Hubland, Würzburg D-97074, Germany*

<sup>2</sup>*Nanoplus GmbH, Oberer Kirschberg 4, Gerbrunn D-97218, Germany*

(Received 1 August 2014; accepted 11 August 2014; published online 21 August 2014)

Single mode distributed feedback (DFB) interband cascade lasers were realized by placing metal gratings laterally to dry etched ridges. A discrete tuning range of 104 nm could be realized on the same gain material by a variation of the grating period. At room temperature, a 2.4 mm long and 9.8  $\mu\text{m}$  wide ridge with as-cleaved facets emitted more than 6 mW of single mode output power in continuous-wave (cw) mode at a wavelength around 3.8  $\mu\text{m}$ . With typical temperature- and current-tuning rates of 0.31 nm/ $^{\circ}\text{C}$  and 0.065 nm/mA, respectively, a total tuning bandwidth of more than 10 nm could be covered with a single device. © 2014 AIP Publishing LLC.

[<http://dx.doi.org/10.1063/1.4893788>]

The mid infrared spectral region (MIR) is of great interest for gas detection since a variety of aliphatic gases like methane, ethane or formaldehyde have rotational-vibrational absorption features in this wavelength region. Tunable laser absorption spectroscopy (TLAS) is a powerful tool in this field which demands compact laser sources that emit in one single longitudinal mode. ICLs<sup>1</sup> are ideally suited for this application as they have several advantages when being compared to conventional diode lasers or quantum cascade lasers (QCLs). They are able to cover the whole spectral range from 3  $\mu\text{m}$  to 6  $\mu\text{m}$  with room temperature continuous wave performance devices.<sup>2,3</sup> Compared to QCLs, they require significantly less power to reach the lasing threshold, which is mostly attributed to the interband carrier lifetime in ICLs, which is about three orders of magnitude longer than the lifetime of intersubband transitions<sup>4</sup> that QCLs make use of. As a result a higher number of cascades is needed in QCLs (typically 30–40) to produce enough gain to overcome the resonator losses and hence the voltage that has to be applied increases. For ICLs threshold power densities of 315 W/cm<sup>2</sup>,<sup>5</sup> threshold current densities lower than 100 A/cm<sup>2</sup> (Ref. 6) and continuous-wave (cw) input powers of 29 mW (Ref. 2) at threshold have been reported. This makes ICLs perfectly suitable for compact systems and portable applications that benefit from longer battery lifetime.

Single mode operation—which is required for gas sensing applications—can be achieved by the incorporation of a wavelength selective grating in the laser resonator. Since epitaxial regrowth is challenging in the GaSb material system, all single mode ICL devices reported up to now use gratings that are added after the epitaxy of a full laser layer. So far, two different overgrowth-free DFB concepts for single mode operation of ICLs have been presented—corrugated sidewalls and Ge top gratings.<sup>7,8</sup> Lasers based on both concepts have already shown impressive performance. However, the single mode yield of corrugated sidewall DFBs is rather low and depends strongly on the quality of the dry etching. If top gratings are used, the thickness of the upper

InAs/AlSb superlattice cladding has to be reduced in order to ensure a sufficient coupling of the laser mode with the grating, which leaves less design freedom for optimal device performance.

Here, we present DFB lasers based on a concept that has already been demonstrated with conventional diode lasers.<sup>9–12</sup> For this purpose metal gratings were patterned laterally to the laser ridge so that the evanescent part of the laser mode couples to the grating, leading to a period modulation of the losses in the resonator. The emission wavelength is then determined by the grating period and the effective refractive index of the laser waveguide. Regarding the coupling strength of the grating several parameters have to be considered. By varying the etch depth, the gratings can be placed at different heights of the waveguide structure. To provide a smooth surface, the GaSb:Te separate confinement layers are predestinated to stop the etch therein. The coupling is stronger when the gratings are placed in the upper SCL, but excessive current spreading and poor heat removal from the sidewalls are drawbacks regarding the laser performance in continuous wave mode. Therefore, the gratings were placed in the lower SCL. The overlap of the fundamental lateral mode displays a linear dependence on the etch depth therein and the thickness of the chromium grating. Additionally, the ridge width plays a significant role for the coupling strength since the overlap increases exponentially when the ridge width is reduced. For ridges wider than 7  $\mu\text{m}$ , the coupling coefficient is expected to be smaller than 5 cm<sup>-1</sup>.<sup>13</sup>

The developed DFB devices are based on 5 stage ICL material grown by MBE on n-GaSb (100) substrates using an EIKO EV-100 system. The active region design is similar to that described in Ref. 2. To shorten the electron injector only 5 instead of 6 InAs quantum wells were grown and the active W-quantum well thicknesses were adjusted in order to achieve laser emission at 3.8  $\mu\text{m}$ . The active region is surrounded by 200 nm thick GaSb:Te separate confinement layers and InAs:Si/AlSb superlattice cladding layers. To evaluate the quality of the epitaxial material, 150  $\mu\text{m}$  wide broad area lasers were processed and characterized electrically in pulsed mode (200 ns pulses, 1 kHz repetition). At 20  $^{\circ}\text{C}$  the threshold current density for a 2 mm long device

<sup>a)</sup>Present address: School of Physics and Astronomy, North Haugh, St Andrews KY16 9SS, United Kingdom.

with uncoated facets was  $151 \text{ A/cm}^2$  and the threshold power density was  $434 \text{ W/cm}^2$  which represents state of the art performance and enables ridge waveguide lasers to emit in cw mode above room temperature. For this purpose narrow ridges of  $7.8 \mu\text{m}$  and  $9.8 \mu\text{m}$  width were defined by optical lithography and a  $\text{BaF}_2/\text{Cr}$  mask and dry etched by an electron cyclotron resonance plasma process. The etch was stopped right after the transition layer that connects the active region and the lower separate confinement layer. Subsequently,  $30 \text{ nm}$  of  $\text{Si}_3\text{N}_4$  were sputtered by plasma enhanced physical vapor deposition to prevent short-circuiting of the active region. First order metal gratings with periods from  $546 \text{ nm}$  to  $574 \text{ nm}$  were then defined by e-beam lithography in Poly(methyl methacrylate) (PMMA) resist, subsequent evaporation of chromium with a thickness of  $110 \text{ nm}$  and a lift-off.

Fig. 1 shows a scanning electron micrograph of the ridge after this process step. To protect the sidewalls, a  $200 \text{ nm}$  thick layer of  $\text{Si}_3\text{N}_4$  was deposited afterwards. Then the mask and the passivation on top of the ridge were removed by a lift-off step in warm water and  $\text{Ti/Pt/Au}$  was evaporated as top contact. For improved heat removal,  $5 \mu\text{m}$  of gold were electroplated on top of the ridge and the substrate was thinned to  $150 \mu\text{m}$ . Finally a  $\text{AuGe/Au}$  contact was evaporated on the substrate side and annealed at  $250^\circ\text{C}$ . For characterization laser bars of  $1.2$  and  $2.4 \text{ mm}$  length were cleaved and mounted epitaxial side up on a copper mount with In-solder. The facets were left as cleaved.

As shown in Fig. 2 single mode operation at room temperature could be observed for grating periods ranging from  $546 \text{ nm}$  to  $562 \text{ nm}$ . For larger grating periods, the mismatch between the gain profile and the Bragg wavelength of the grating resulted in multimode operation. In the  $3.8 \mu\text{m}$  wavelength region, a spectral range of more than  $100 \text{ nm}$  is accessible for single mode operation with one epitaxial structure. The full discrete tuning width could be observed for both ridge widths, indicating sufficient coupling to the grating. From the wavelength and the grating period, the modal index was estimated to  $3.45$  at room temperature, which perfectly matches the theoretically calculated value. In Fig. 3, the

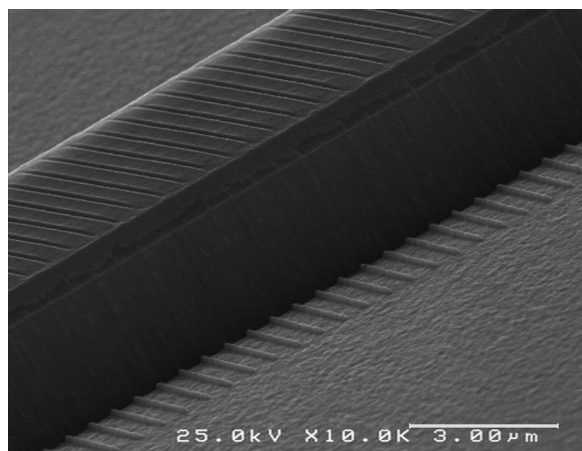


FIG. 1. Scanning electron micrograph of an ICL ridge with laterally patterned chromium gratings before passivation and lift off. The grating is very accurate which is mandatory for good coupling especially close to the sidewalls.

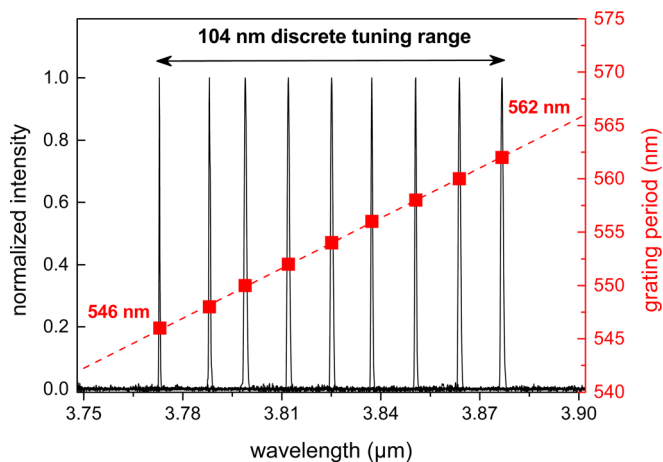


FIG. 2. Single mode spectra for different grating periods ranging from  $546 \text{ nm}$  to  $562 \text{ nm}$  at a driving current of  $100 \text{ mA}$  (device dimensions:  $2.4 \text{ mm} \times 9.8 \mu\text{m}$ ).

single mode current tuning for several temperatures is displayed for a laser ridge with  $548 \text{ nm}$  grating period. With temperature and current tuning rates of  $0.31 \text{ nm}/^\circ\text{C}$  and  $0.065 \text{ nm}/\text{mA}$ , respectively, a total tuning range of over  $10 \text{ nm}$  could be realized for the  $2.4 \text{ mm}$  long device. The temperature tuning rate for  $1.2 \text{ mm}$  long devices were larger with typical values around  $0.079 \text{ nm}/\text{mA}$ . This effect is based on the poorer heat spreading in short devices and facilitates faster wavelength modulation. The inset in Fig. 3 shows single mode spectra for various temperatures and a driving current of  $100 \text{ mA}$  measured with a Bruker Fourier transform infrared spectrometer (resolution:  $0.12 \text{ cm}^{-1}$ ) in rapid scanning mode. The side mode suppression ratio (SMSR) is higher than  $30 \text{ dB}$ . The noise features exceeding this level originate from the FTIR measurement. In Fig. 4, the light-current-voltage characteristics are displayed for the  $2.4 \text{ mm}$  long and  $9.8 \mu\text{m}$  wide ridge with uncoated facets. Single mode operation with at least  $30 \text{ dB}$  SMSR could be maintained from threshold to at least  $110 \text{ mA}$  in a temperature range from  $10^\circ\text{C}$  to  $35^\circ\text{C}$ . At  $20^\circ\text{C}$ , the threshold current and power were  $70 \text{ mA}$  and  $203 \text{ mW}$ , respectively, which is considerably lower than for the best reported QCLs in this

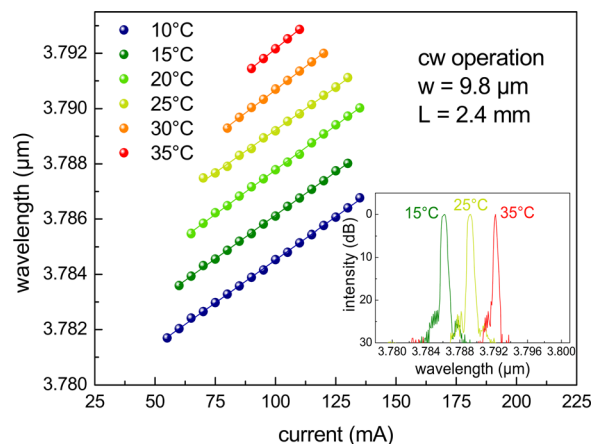


FIG. 3. Temperature and current tuning characteristics of a  $9.8 \mu\text{m}$  wide and  $2.4 \text{ mm}$  long ICL-DFB device. Single mode spectra with more than  $30 \text{ dB}$  side mode suppression ratio are shown in the inset for  $T = 15^\circ\text{C}/25^\circ\text{C}/35^\circ\text{C}$  at a driving current of  $100 \text{ mA}$ .

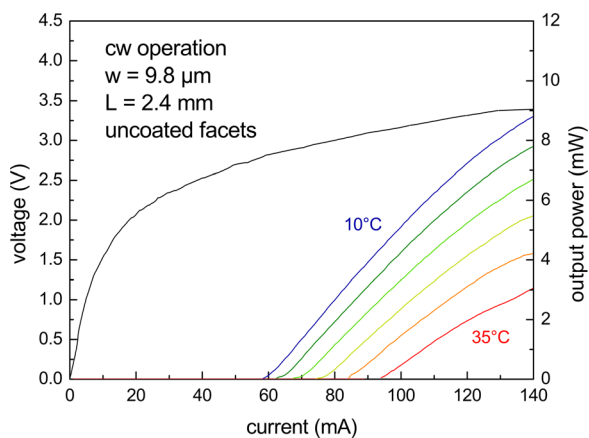


FIG. 4. Light-current-voltage characteristics for a single mode ICL device operated in cw at several temperatures. The IV-characteristic was measured at 20 °C. (device dimensions: 2.4 mm  $\times$  9.8  $\mu$ m).

wavelength region.<sup>14</sup> Furthermore, more than 6 mW of single mode output power were emitted from one facet at 20 °C which is sufficient for most sensing applications. A simple way of increasing the output power would be a combination of high-reflective and anti-reflective facet coating.

We successfully realized laterally coupled DFB lasers with metal gratings based on 5 stage IC gain material. For that purpose chromium gratings were patterned laterally to a dry etched ridge via e-beam lithography and a lift-off step. The position of the grating relative to the waveguide structure was found to be critical for the coupling strength and hence the single mode yield and tuning width. A total temperature-current tuning width of more than 10 nm could be realized for a 2.4 mm long and 9.8  $\mu$ m wide ridge. At room temperature the device emitted more than 6 mW of single mode output power in cw mode and the power consumption at threshold was only 203 mW. Via optimized coupling strength and appropriate facet coatings the output power can

be increased even further. Since ICLs operate in cw mode at room temperature in a wide spectral range (3 to 6  $\mu$ m)<sup>3</sup> the presented concept can be applied throughout the mid infrared region by simply adjusting the grating period and position.

We are very grateful to the European Union for financial support of this work within the FP7 project “WideLase” (No. 318798). We also would like to thank S. Kuhn, M. Wagenbrenner, S. Handel, and T. Steinel for assistance during sample preparation, growth, and characterization and M. Dallner for fruitful discussions.

- <sup>1</sup>R. Q. Yang, *Superlatt. Microstruct.* **17**(1), 77 (1995).
- <sup>2</sup>I. Vurgaftman, W. W. Bewley, C. L. Canedy, C. S. Kim, M. Kim, C. D. Merritt, J. Abell, J. R. Lindle, and J. R. Meyer, *Nature Commun.* **2**, 585 (2011).
- <sup>3</sup>W. W. Bewley, C. L. Canedy, C. S. Kim, M. Kim, C. D. Merritt, J. Abell, I. Vurgaftman, and J. R. Meyer, *Opt. Express* **20**(3), 3235 (2012).
- <sup>4</sup>I. Vurgaftman, W. W. Bewley, C. L. Canedy, C. S. Kim, M. Kim, C. D. Merritt, J. Abell, and J. R. Meyer, *IEEE J. Select. Top. Quantum Electron.* **19**(4), 1200210 (2013).
- <sup>5</sup>W. W. Bewley, C. L. Canedy, C. S. Kim, M. Kim, C. D. Merritt, J. Abell, I. Vurgaftman, and J. R. Meyer, *Opt. Express* **20**(19), 20894 (2012).
- <sup>6</sup>R. Weih, S. Höfling, and M. Kamp, *Appl. Phys. Lett.* **102**, 231123 (2013).
- <sup>7</sup>C. S. Kim, M. Kim, W. W. Bewley, J. R. Lindle, C. L. Canedy, J. Abell, I. Vurgaftman, and J. R. Meyer, *Appl. Phys. Lett.* **95**, 231103 (2009).
- <sup>8</sup>C. S. Kim, M. Kim, J. A. Bell, W. W. Bewley, C. D. Merritt, C. L. Canedy, I. Vurgaftman, and J. R. Meyer, *Appl. Phys. Lett.* **101**, 061104 (2012).
- <sup>9</sup>M. Kamp, J. Hofmann, A. Forchel, F. Schäfer, and J. P. Reithmaier, *Appl. Phys. Lett.* **74**, 483 (1999).
- <sup>10</sup>M. Kamp, J. Hofmann, F. Schäfer, M. Reinhard, M. Fischer, T. Bleuel, J. P. Reithmaier, and A. Forchel, *Opt. Mater.* **17**, 19–25 (2001).
- <sup>11</sup>J. Seufert, M. Fischer, M. Legge, J. Koeth, R. Werner, M. Kamp, and A. Forchel, *Spectrochim. Acta Part A* **60**, 3243–3247 (2004).
- <sup>12</sup>L. Naehle, S. Belahsene, M. von Edlinger, M. Fischer, G. Boissier, P. Grech, G. Narcy, A. Vicet, Y. Rouillard, J. Koeth, and L. Worschech, *Electron. Lett.* **47**(1), 46 (2011).
- <sup>13</sup>Y. B. Wang, Y. Xu, Y. Zhang, G. F. Song, and L. H. Chen, *J. Phys. D* **45**, 505109 (2012).
- <sup>14</sup>N. Bandyopadhyay, Y. Bai, B. Gokden, A. Myzaferi, S. Tsao, S. Slivken, and M. Razeghi, *Appl. Phys. Lett.* **97**, 131117 (2010).